



ELSEVIER

Contents lists available at ScienceDirect

Thermochimica Acta

journal homepage: www.elsevier.com/locate/tca



Application of evolved gas analysis to cold-cap reactions of melter feeds for nuclear waste vitrification

Carmen P. Rodriguez^a, Jaehun Chun^{a,*}, Michael J. Schweiger^a, Albert A. Kruger^b, Pavel Hрма^{a,c}

^a Pacific Northwest National Laboratory, 902 Battelle Blvd., P.O. Box 999, MSIN K6-24, Richland, WA 99352, USA

^b U.S. Department of Energy Office of River Protection, Richland, WA 99352, USA

^c Division of Advanced Nuclear Engineering, Pohang University of Science and Technology, Pohang, Republic of Korea

ARTICLE INFO

Article history:

Received 20 August 2013

Received in revised form 20 June 2014

Accepted 23 June 2014

Available online xxx

Keywords:

Cold-cap reactions

Evolved gas analysis

Nuclear waste vitrification

Kinetic models

ABSTRACT

In the vitrification of nuclear wastes, the melter feed (a mixture of nuclear waste and glass-forming and modifying additives) experiences multiple gas-evolving reactions in an electrical glass-melting furnace. We employed the thermogravimetry–gas chromatography–mass spectrometry (TGA–GC–MS) combination to perform evolved gas analysis (EGA). Along with identifying the gases evolved, we performed quantitative analysis relating the weighted sum of intensities of individual gases in linear proportion with the differential thermogravimetry. The proportionality coefficients were obtained by three methods based on the stoichiometry, least squares, and calibration. The linearity was shown to be a good first-order approximation, in spite of the complicated overlapping reactions.

© 2014 Elsevier B.V. All rights reserved.

1. Introduction

The cold cap is a floating layer of melter feed, or glass batch, on a pool of molten glass in a continuous electrical glass-melting furnace, termed a melter. For vitrifying nuclear waste glass [1–3], the feed, a mixture of waste with glass-forming and -modifying additives, is charged onto the cold cap that covers 90–100% of the melt surface. As the feed moves through the cold cap, it undergoes chemical reactions and phase transitions, through which it is converted to molten glass that moves from the cold cap into the melt pool.

The nuclear waste (i.e., mixed hazardous waste) contains 40–60 elements forming water-soluble salts, amorphous gels, and crystalline minerals. The conversion to glass proceeds over a wide range of temperatures (~100–1100 °C) spanning the formation of molten salts that react with feed solids, turning them into intermediate products and ultimately the glass-forming melt. Various cold-cap reactions evolve gases that escape from the cold cap through open pores. A small fraction of residual gases can be trapped in the glass-forming melt and cause foaming. Foam reduces the heat transfer from the molten glass into the cold cap, decreasing the rate of melting. Understanding the cold-cap reactions over the temperature range of the conversion process

helps formulate melter feeds for higher production rates, and hence an enhanced efficiency of the vitrification facility, by minimizing the overlap between the gas-evolving reactions and the formation of a highly viscous continuous glass-forming melt.

Gas-evolving cold-cap reactions release chemically bonded water and produce NO_x, O₂, and CO_x from reactions of nitrates with organics and reactions of nitrates, nitrites and carbonates with solids [4–17]. Pokorný et al. [3] modeled the kinetics of the gas-evolving cold-cap reactions using data from non-isothermal thermogravimetric analysis (TGA). Their model described the overall reaction rate as a sum of mutually independent *n*th-order reaction kinetics with the Arrhenius rate coefficients. For simplification, they neglected interactions between consecutive reactions and the complex responses of multicomponent molten salts and other reactants. Chun et al. [18] used a similar approach to develop a kinetic model for heat-consuming cold-cap reactions from simultaneous differential scanning calorimetry (DSC)-TGA data. It should be noted that reaction peaks identified in both approaches could result from the combination of sub-reactions in a similar temperature range unless the mixtures are treated at a wide range of heating rates.

The TGA- and DSC-based kinetic models provide phenomenological descriptions of the cold-cap reactions. Given the complexity of nuclear waste feeds and glass batches in general, these methods do not identify chemical species involved. Neither does the evolved gas analysis (EGA), but it does at least allow the

* Corresponding author. Tel.: +1 509 372 6257; fax: +1 509 372 5997.
E-mail address: jaehun.chun@pnnl.gov (J. Chun).

gases evolved to be recognized. Previous informative, yet semi-quantitative, EGA studies [19,20] analyzed off-gases from a laboratory-scale furnace without attempting to determine contributions of each of the gases to the mass losses. In this study, we correlate the mass loss rate from TGA with the well-resolved fluxes of gases as detected by gas chromatography–mass spectrometry (GC–MS) to obtain a quantitative EGA. The resulting model provides contributions of individual gases to mass losses associated with the feed-to-glass conversion.

The following section defines the basic concepts and relationships. Sections 3 and 4 describe the experiments and the results. Section 5 discusses the performance and applicability of the model as well as the prospective deeper characterization of feed melting reactions. In addition, the correspondence between the crucible experiments and the large-scale melting process from the viewpoint of sample preparation is examined.

2. Background for modeling

Assuming that the mass loss of the batch is only associated with gas evolution reactions [3], the change of the TGA sample mass equals the sum of mass changes of gases evolved. Thus,

$$-\frac{dm}{dt} = \sum_{j=1}^{N_g} \frac{dm_j}{dt} \quad (1)$$

where m is the sample mass, m_j is the j th off-gas mass, N_g is the number of gas species, and t is time. This assumption is reasonable for alkali-borosilicate batches for temperatures $< \sim 800^\circ\text{C}$; above this temperature, volatilization losses become appreciable.

For analysis with GC–MS, the flux of the j th gas species, represented via intensity, I_j , is proportional to the flux of molecular ions (or instrumentally produced current). Thus, $dm_j(t)/dt = F_j I_j(t')$, where F_j is the j th off-gas proportionality coefficient and $t' = t - \Delta t$; Δt is the time lag between the TGA signal and the MS detector reading due to the off-gas transfer to the MS detector. The dimension of F_j is such that the $F_j I_j$ product, which defines the j th gas production rate, has an appropriate [mass/time] unit. Eq. (1) then becomes:

$$-\frac{dm(t)}{dt} = \sum_{j=1}^{N_g} F_j I_j(t') \quad (2)$$

Provided that F_j and Δt are constant on the temperature interval of gas evolution, Eq. (2) can be integrated, obtaining:

$$\Delta m = \sum_{j=1}^{N_g} F_j \int_0^{t_f} I_j(t') dt \quad (3)$$

where Δm is the total mass loss measured by the TGA instrument and t_f is the time at which the gas evolution was complete (i.e., the time where the mass of the final glass can be defined via the remaining sample mass). The F_j coefficients can be obtained by fitting Eq. (2) to TGA–EGA data (see Section 4).

Generally, various factors need to be considered for a correlation between TGA and MS signals, such as flow patterns in the TGA chamber and carrier gas flow rates [21,22]. Eq. (2) (and thus Eq. (3)) would not be applicable in the presence of interfering experimental artifacts and/or a strong coupling of the reaction evolving the j th off-gas with other reactions (e.g., the gas consumed by other reactions). However, the implementation of the GC column (i.e., the affinity of gas species to a stationary phase inside the GC column) and the small volume of the GC injector may sufficiently reduce the broadening of the MS peaks to allow Eq. (2) to be a reasonable approximation (see Section 3.2 and Fig. 2).

The integral form of Eq. (1) can be written as:

$$\Delta m = \sum_{j=1}^{N_g} \Delta m_j \quad (4)$$

where Δm_j is the mass loss due to the j th off-gas. Comparing Eq. (3) with Eq. (4), we obtain:

$$F_j = \frac{\Delta m_j}{\int_0^{t_f} I_j(t') dt} \quad (5)$$

The mass fraction of the j th gas that evolved per unit mass of dry feed is defined as:

$$w_{F_j} = \frac{\Delta m_j}{m} \quad (6)$$

Note that w_{F_j} was marked as w_j in [3]. The total gas-to-dry feed mass fraction is:

$$w_F = \sum_{j=1}^{N_g} w_{F_j} = \frac{\Delta m}{m} \quad (7)$$

Combining Eqs. (5) and (6), we obtain:

$$w_{F_j} = \frac{F_j}{m} \int_0^{t_f} I_j(t') dt \quad (8)$$

Assuming that the intensity response only depends on the nature of the gas, Eqs. (3), (5), and (8) are valid with identical values of F_j and Δt for any set of gas evolving reactions that are complete within the given interval of temperatures provided that the same instrument and experimental conditions are applied. Consequently, it is possible to calibrate the instrument for individual gases using solid samples that release a single gas in a single reaction. Then,

$$\Delta m_j = C_j \int_0^{t_f} I_j dt \quad (9)$$

where C_j is the j th gas calibration coefficient [23]. It follows from Eqs. (5) and (9) that $F_j = C_j$ for $j = 1, \dots, N_g$. To obtain a reliable calibration coefficient, three samples of a simple solid substance are typically analyzed to minimize experimental errors.

Table 1
Melter feed composition for high-alumina high-level waste in g kg^{-1} glass.

Chemicals	Mass (g)
Al(OH) ₃	367.50
H ₃ BO ₃	269.83
CaO	60.80
Fe(OH) ₃	73.83
Li ₂ CO ₃	88.30
Mg(OH) ₂	1.70
NaOH	99.53
SiO ₂	305.03
Zn(NO ₃) ₂ ·4H ₂ O	2.67
Zr(OH) ₄ ·0.654H ₂ O	5.50
Na ₂ SO ₄	3.57
Bi(OH) ₃	12.80
Na ₂ CrO ₄	11.13
KNO ₃	3.03
NiCO ₃	6.33
Pb(NO ₃) ₂	6.17
Fe(H ₂ PO ₄) ₃	12.43
NaF	14.73
NaNO ₂	3.40
Na ₂ C ₂ O ₄ ·3H ₂ O	1.30
Total	1349.6

3. Experimental

3.1. Feed materials

Table 1 shows the melter feed composition used in this study. As described previously [3,18,24], this feed, denoted as A0, was formulated to vitrify a high-alumina high-level waste to produce glass of the following composition (with mass fractions in parentheses): SiO₂ (0.305), Al₂O₃ (0.240), B₂O₃ (0.152), Na₂O (0.096), CaO (0.061), Fe₂O₃ (0.059), Li₂O (0.036), Bi₂O₃ (0.011), P₂O₅ (0.011), F (0.007), Cr₂O₃ (0.005), PbO (0.004), NiO (0.004), ZrO₂ (0.004), SO₃ (0.002), K₂O (0.001), MgO (0.001), and ZnO (0.001). This glass was designed for the Hanford Tank Waste Treatment and Immobilization Plant, currently under construction at the Hanford Site in Washington State, USA [25]. As described by Schweiger et al. [24], the simulated melter feed was prepared in the form of slurry that was dried, crushed into powder, and placed in an oven at ~105 °C overnight. As discussed in Section 5.3, the slurry feed was used, instead of the direct mixing and melting batched chemicals, to simulate the actual melter feed as closely as practicable, even though subsequent drying and storing operation produce secondary effects of exchange of gases with the atmosphere. As shown below, EGA made it possible to discern these effects.

3.2. TGA-GC-MS system

In the study, we used a simultaneous TGA-GC-MS coupled system consisting of a NETZSCH STA 449 F1 Jupiter[®] Simultaneous TGA-DSC instrument simultaneously coupled to an Agilent 7890A gas chromatograph equipped with an Agilent 5975C single quadrupole mass spectrometer. Evolved gases moved directly from the TGA chamber using helium as a carrier gas (under atmospheric pressure) to the GC-MS via heated transfer tubing. Evolved gases flowed through the GC sampling loop, and, in every minute, a partitioned segment was injected into the GC column, eluted with helium gas, and the gases were speciated by the GC before they entered the MS detector for analysis. Unlike a conventional capillary coupling, the stationary phase in the GC, along with a small injection volume, provided different interactions with each gas in the mixture, allowing a better resolution (i.e., avoiding significant broadening of the peaks in the MS).

The TGA instrument temperature and sensitivity were calibrated, following the manufacturer guidelines. To check for leaks, impurities, and residues from TGA/GC and peripheral setups (e.g., pumps and valves), multiple 'blank' runs without a sample were performed at the heating rate of 10 K min⁻¹ from 50 °C to 1200 °C.

The EGA was begun by placing 61.7 mg of the sample, prepared following the procedure in Section 3.1, into a platinum crucible. After loading the crucible into the TGA furnace, the instrument was stabilized, following manufacturer guidelines, by flowing helium through the system a couple of times. Simultaneously, to reduce background noises, the GC-MS instrument was stabilized by flowing helium through the system for 2–3 h and then run for about 10 min. As the open crucible with the sample was heated at 10 K min⁻¹ from 50 °C up to 1200 °C, helium was used as both a purge gas (at a constant flow rate of 20 ml min⁻¹) and protective gas (at a constant flow rate of 40 ml min⁻¹). The GC injector was set to splitless mode. The GS-CarbonPLOT capillary column, specifically designed for low molecular weight gas molecules, such as N₂, CH₄, CO₂, N₂O, and H₂O, was 30 m long and 320 μm in inner diameter and possessed a 3-μm film thickness. The GC-MS instrument ran under a helium atmosphere with a constant column flow rate of 1.5 ml min⁻¹. To avoid possible condensation, the valve box (containing a 250 μl sampling loop), the transfer tubing, and the GC column were held at a high enough temperature (>100 °C). The reproducibility was checked at the optimized setting

conditions (i.e., temperature, size of crucible, and flow rates specified) multiple times. Data were collected from TGA and GC-MS at the intervals of ~0.5 min and ~1 min, respectively.

The National Institute of Standards and Technology (NIST) mass spectral database [26], containing a collection of electron ionization mass spectra for various molecular species, was employed to identify evolved gases. For the MS, ionization energy was set to 20 eV, the scan range m/z (mass-to-charge ratio) was 10–100, and the the GC-MS interface was set to 280 °C.

4. Results

Fig. 1 shows the normalized mass loss (TG), its time derivative (DTG), and intensity from GC-MS. The four gases, CO₂, H₂O, NO, and O₂, were identified by matching observed m/z patterns in MS with the NIST spectroscopy library database.

Fig. 1(b) displays the intensity in arbitrary units obtained as the MS signal multiplied by 10⁻⁶, which is applied for all results in our study. Note that it determines the order of magnitude of F_j (and C_j) because the $F_j I_j$ (and $C_j I_j$) product should provide the same j th gas production rate, irrespective of such normalization. As shown in Fig. 1(b), the major gases are CO₂ and H₂O with significant overlapping. The minor NO peak and the tiny O₂ peak coincide with the major peak of CO₂ while H₂O continues to evolve. The first DTG peak seen in Fig. 1(a) at ~10 min (~150 °C) did not occur in the DTG results reported in our previous study [3]. We attributed this peak to the release of excess water accumulated in the sample by adsorption (also reported by Krämer [17]) and capillary condensation of atmospheric moisture.

To match the DTG and GC-MS temperature scales, data were smoothed with spline interpolation and a 1.5-min time lag was applied. The time lag of the off-gas transfer from TGA to MS detector corresponds to the 1.5-ml min⁻¹ flow rate through the transfer line and the 30-m GC column with 320 μm inner diameter.

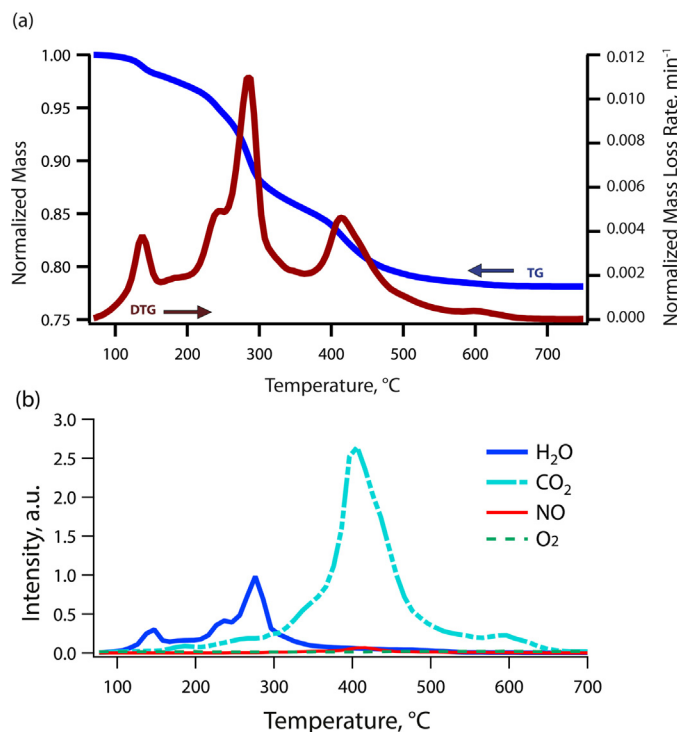


Fig. 1. (a) Dry feed TGA performed at 10 K min⁻¹; TG is the normalized mass based on initial sample mass and DTG is the time derivative of the normalized mass (equivalently, the normalized mass loss rate) and (b) the intensity from GC-MS.

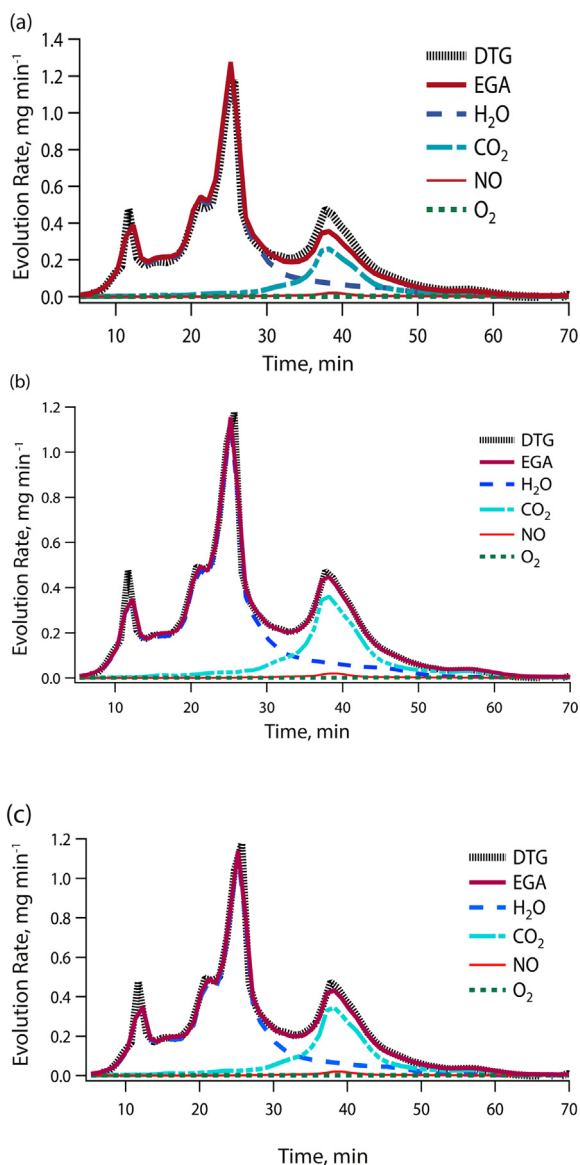


Fig. 2. Gas evolution rates for gaseous species by TGA and GC-MS with the proportionality coefficients from three different methods: (a) stoichiometry method, (b) least squares method, and (c) calibration method.

The TGA measured value of the total gas-to-dry feed mass fraction, defined by Eq. (7), is $w_F = 0.2158$, see Fig. 1(a). This value favorably compares with the average value from the previous study [3], which was 0.2023 ± 0.0029 . The experimental value of the loss on ignition obtained from an independently prepared feed was 0.1917. These values are close, considering uncertainties associated with feed preparation, aging, and the small sample size used for thermal analysis.

Expressing the content of sample constituents in terms of mass fractions related to the initial dry-feed sample is convenient for TGA and DSC studies [3,18]. Relating the mass fractions to the final glass is convenient for application to the vitrification process, where the main focus is on the product. The mass loss from dry feed per unit mass of glass is $w_G = \Delta m/m_G = w_F/(1 - w_F) = 0.2751$.

In principle, proportionality coefficients (F_{js}) can be determined by the stoichiometry method, least squares method, and calibration method. The stoichiometry method identifies Δm_j with the amount of gas that would be released from the batch chemicals

provided that no j th gas was evolved from, or received by, the sample during feed preparation and storage. This method can be applied to feed constituents that are sufficiently stable, such as nitrates and nitrites, evolving NO and O₂. However, as expected, bonded water was partially liberated during feed preparation and some water and CO₂ were taken up from the atmosphere during dry feed storage, though simultaneous loss of water by slow room-temperature reactions cannot be ruled out.

The least squares method is based on fitting Eq. (2) to DTG and EGA data using least squares regression. This method is limited to gas-evolving reactions that are independent and do not have coincident peaks. As Fig. 1(b) indicates, this is not the case for the NO and O₂ peaks, which are eclipsed by the CO₂ peak. Finally, the calibration method uses a solid subjected to a single gas-evolving reaction in order to obtain the C_j coefficients (by Eq. (4)) as the F_{js} . This method should work for all gases but needs to be checked with the other two methods.

The following subsections describe the application of the three methods to experimental data. The common source of uncertainty is that the small size of the sample containing a large number of components can cause composition deviations.

4.1. Stoichiometry method

The amounts of gases that evolve from the batch chemicals (listed in Table 1) during the vitrification process can be obtained based on the stoichiometry of batch reactions involved in the conversion of the batch chemicals and minerals (Table 1) to molten glass (Section 3.1). The mass loss associated with this process is the result of the release of the volatile components, such as H₂O and CO₂, to the atmosphere. Thus, the mass fraction of the j th gas evolved from the original batch per unit mass of glass is defined as the mass of the j th gas, ($\Delta m_{B,j}$) released from the chemicals batched per the mass of glass produced (m_G):

$$w_{B,j} = \frac{\Delta m_{B,j}}{m_G} \quad (10)$$

Clearly, $m_G = m_B - \Delta m_B$, where m_B is the total mass of chemicals batched to make glass (listed in Table 1) and Δm_B is the total mass of all gases evolved, $\Delta m_B = \sum_{j=1}^{N_g} \Delta m_{B,j}$. The subscript B stands for

batched chemicals. Based on the batched composition listed in Table 1, stoichiometric calculation allows us to obtain the following $w_{B,j}$ values: $w_{B,CO_2} = 0.0558$, $w_{B,NO} = 0.0041$, $w_{B,O_2} = 0.0023$, and $w_{B,H_2O} = 0.2871$. The summation of these values is the total mass loss from batched chemical per glass $w_B = 0.3493$.

Generally, considering the sample preparation mentioned in Section 3.1, $w_{B,j}$ consists of three contributions: the fraction released or acquired during sample preparation ($w_{j,p}$), the fraction released or acquired during sample storage ($w_{j,s}$), and the fraction released during conversion reactions ($w_{j,h}$):

$$w_{B,j} = w_{j,p} + w_{j,s} + w_{j,h} \quad (11)$$

Thus, the actual mass loss from dry feed per unit mass of glass (as measured by the EGA of the dry feed sample), $w_G = \sum_{j=1}^{N_g} w_{j,h}$, is lower

than w_B unless $w_{j,p} = w_{j,s} = 0$ for all gases. Since $w_G = \Delta m/m_G$, we obtain $w_G = w_F/(1 - w_F) = 0.2751$, which is indeed significantly lower than w_B .

As stated above, F_{js} for NO and O₂ can be safely estimated based on the stoichiometry of the batch chemicals because these gases are neither released to nor absorbed from the atmosphere during sample preparation. Hence, for $j = \text{NO}$ and O₂, $w_{j,p} = w_{j,s} = 0$ and

Table 2

Proportionality coefficients of H₂O and CO₂, CO₂ gas evolved per unit mass of dry feed, and calculated total gas-to-dry feed mass fraction based on three methods.

Method	F_{H_2O}	F_{CO_2}	w_{F,CO_2}	w_F
Stoichiometry	1.280	0.099	0.0437	0.2751
Least squares	1.150	0.136	0.0603	0.2748
Calibration	1.140	0.131	0.0590	0.2701

thus $w_{B,j} = w_{j,h}$. Since $w_{F,j} = w_{j,h}/(1 + w_G)$, we obtain $w_{F,NO} = 0.0032$, and $w_{F,O_2} = 0.0018$.

As mentioned, not all bonded water from the batched chemicals is retained in the dry feed. Some originally bonded water was liberated during feed preparation, especially drying, due to water-releasing chemical reactions. Also, some water was acquired from the atmosphere during dry feed storage or slowly lost by continuing reactions. Hence, $w_{H_2O,p}$ and $w_{H_2O,s}$ can be substantial.

Assuming, for simplicity, that the difference between w_B and w_F is solely attributed to H₂O and the only sources of CO₂ in the sample are the oxalate and carbonates from the batch, we obtain $w_{F,CO_2} = 0.0437$. The difference between w_F and the sum of the $w_{F,j}$ values for NO, O₂, and CO₂ then equals $w_{F,H_2O} = 0.1670$.

By Eq. (8), $F_j = mw_{F,j} / \int_0^t I_j dt$. Performing the numerical integration and using the $w_{F,j}$ values shown above, we obtain the stoichiometry-based values $F_{NO} = 0.297$ and $F_{O_2} = 0.0693$; the F_j values for H₂O and CO₂ are listed in Table 2.

Fig. 2(a) displays the evolution rates of individual gases as well as the sum of all gases, which is compared with the mass loss rate by the TGA. The EGA and TGA curves nearly coincide at $t < \sim 30$ min, indicating that the F_{H_2O} coefficient has an acceptable value. A substantial lack of fit for the peak to which CO₂ is a dominant contributor indicates that the CO₂ fraction in the sample was higher than that which came from the batch chemicals. The most likely cause was CO₂ absorption from the atmosphere by the highly alkaline feed.

4.2. Least squares method

The underestimated F_{CO_2} coefficient poses a question regarding the assumption that batch chemicals were the only sources of CO₂ in the sample. However, without this assumption, it is impossible to obtain F_j s for H₂O and CO₂ independently based on stoichiometry. Alternatively, F_{H_2O} and F_{CO_2} coefficients can be obtained by using the least squares analysis while leaving F_{NO} and F_{O_2} from the stoichiometry method unchanged. The analysis minimizes the value of the expression

$$\sum_{i=1}^n \left[\frac{dm(t)}{dt} - \sum_{j=1}^{N_g} F_j I_j(t) \right]^2 \quad (12)$$

where n is the number of GC–MS data measured (typically less than that from TGA – see Section 3.2 for time intervals of data collection). The optimized values of the F_{H_2O} and F_{CO_2} coefficients are listed in Table 2, showing that the fitted F_{CO_2} value is higher than that obtained based on the feed stoichiometry. As Fig. 2(b) demonstrates, the EGA and TGA curves based on the coefficients by the least squares method nearly coincide.

4.3. Calibration method

Additionally, a calibration based on single solid substances producing H₂O and CO₂, i.e., giving coefficients C_{H_2O} and C_{CO_2} , can approximate the F_{H_2O} and F_{CO_2} coefficients. Fig. 3 displays the TGA–GC–MS analysis for a CaCO₃ sample (evolving CO₂ by the

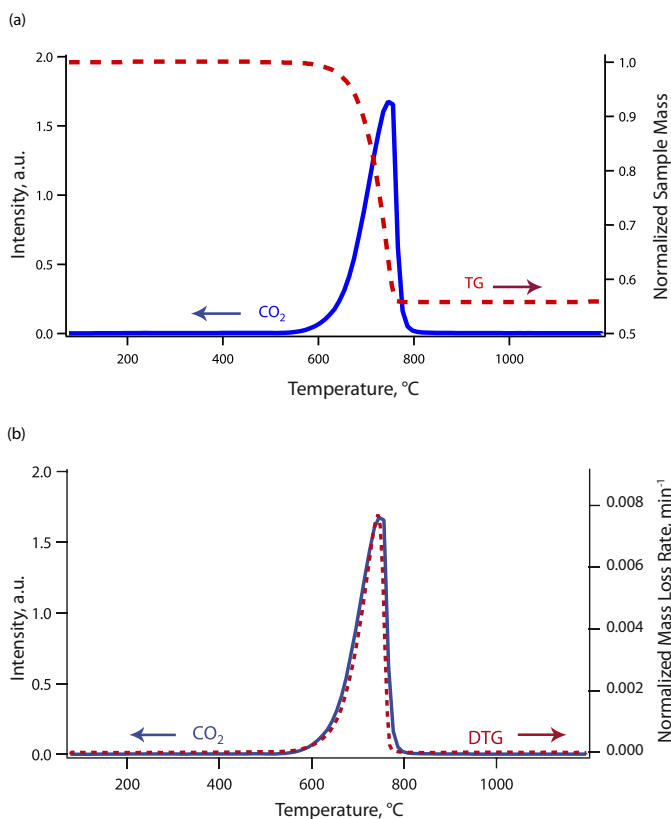


Fig. 3. Thermal decomposition of CaCO₃ heated at 10 K min⁻¹: (a) normalized sample mass and (b) normalized mass derivative or mass loss rate (from TGA) with the intensity (from MS) as a function of temperature.

reaction CaCO₃ → CaO + CO₂) heated at 10 K min⁻¹. The value $C_{CO_2} = 0.131$ was obtained by averaging from samples with 15.4 and 20.7 mg. Similarly, for calcium oxalate monohydrate (CaC₂O₄·H₂O → CaC₂O₄ + H₂O) with 3.0, 4.8, and 9.3 mg samples, $C_{H_2O} = 1.140$ was obtained. These coefficients are compared in Table 2 with the coefficients based on stoichiometry (assuming zero external source of CO₂, NO, and O₂) and the least squares analysis (assuming zero external sources or sinks of NO and O₂).

Fig. 2(c) shows the comparison between DTG and EGA curves using the calibration method. Similar to the least squares method, the discrepancy between the EGA and TGA is minimal even in the

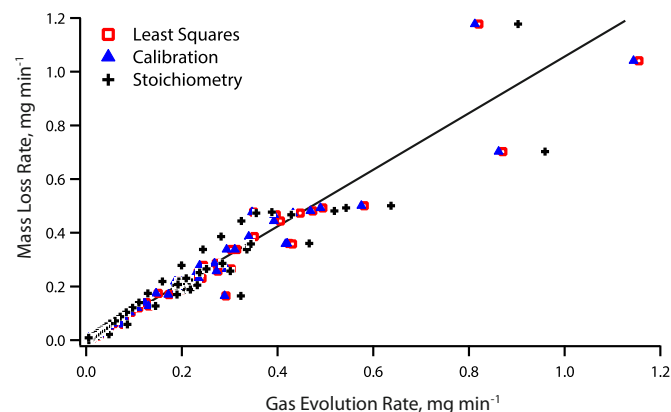


Fig. 4. Instantaneous mass loss rate versus gas evolution rate estimated by the stoichiometry, least squares, and calibration methods; the line represents identity.

major overlapping range (i.e., 30–50 min). Also, as the last column in Table 2 indicates, the difference in the total mass evolved relative to the TGA was insignificant.

Fig. 4 provides an additional evaluation of the proportionality assumption in terms of the instantaneous mass change rate by DTG versus the gas evolution rate by EGA showing that these rates nearly coincide except for values around sharp major peaks where EGA data were not detected (note that the EGA lines in Fig. 2 connect data points spaced ~1 min apart – see Section 3.2).

5. Discussion

5.1. Coefficient invariance

The results summarized in Table 2 imply that the following assumptions are likely to be valid:

- F_j coefficients are virtually independent of temperature.
- F_j coefficients are independent of the gas source.
- The time lag, Δt , is virtually constant over the gas-evolution temperature interval.

The near-match of DTG and EGA peak shapes and positions are consequences of these propositions, in addition to the minimization of experimental artifacts, such as the condensation of evolved gases and impurities from TGA/GC and peripheral setups. Thus, Eq. (2) is suitable as a first-order approximation. The proportionality assumptions stated, though based on a limited amount of data, may help optimize formulation of feeds for nuclear waste vitrification.

5.2. Identification of batch reactions

The previously reported TGA analysis [3] was solely focused on reaction kinetics. Identifying the gases by EGA provides a step toward the identification of the gas-evolving reactions for individual TGA peaks with the ultimate goal of understanding the reaction mechanisms; however, this can only be accomplished using different analytical tools. As Fig. 1 shows, the TGA peaks for individual gases overlap. By EGA results, the TGA peaks below 400 °C mainly correspond to H₂O evolution and the TGA peaks above 400 °C correspond to CO₂ evolution while H₂O is still evolving.

The missing information is the identification of the reactants and the products. While the EGA can add the chemical characteristics to the peaks identified in the TGA, it cannot differentiate between individual reactions that produce the same gas. An exact number of H₂O-evolving reactions would be also more than the number of peaks in Fig. 1. Based on the feed composition in Table 1, H₂O is released from hydroxides, acids, and hydrates, such as NaOH, H₃BO₃, Al(OH)₃, Fe(OH)₃, Zn(NO₃)₂·4H₂O, Zr(OH)₄·0.654H₂O, Na₂C₂O₄·3H₂O, and Bi(OH)₃. NaOH is likely to react with more acidic feed chemicals, such as H₃BO₃ and Al(OH)₃, in the slurry (pH ~11–12) [27,28]. Similarly, the TGA peaks above 400 °C are associated with reactions of carbonates, such as Li₂CO₃, NiCO₃, and Na₂C₂O₄ that may partly turn to Na₂CO₃ on heating.

Performing TGA and EGA for combinations of selected feed components, as Wilburn and Thomasson [4–7] have done for commercial glass batches, can indicate possible reactions in batches with a small number of well-defined components. X-ray diffraction can provide limited data about crystalline solids; however, as most of the feed solids form amorphous gels in the early stages of conversion, a host of methods is needed for understanding the conversion process for even a simplified melter feed [28].

5.3. Connection to vitrification of nuclear wastes in large-scale melters

Whereas the form of chemicals used to make glass have little impact on glass properties, experimental studies focused on vitrification technology require careful preparation of melter feeds to replicate as closely as possible the conversion process occurring in melters. However, exactly replicating the history of the nuclear waste since its creation, including decades-long aging in some cases, is neither possible nor necessary. Slurry-feed preparation described by Schweiger et al. [24] is deemed sufficient.

In U.S. vitrification plants, the slurry feed is directly charged into the melter, where it is transformed to molten glass. For experiments conducted with laboratory crucibles, the slurry is instead dried before the heat treatments. In addition to avoiding boiling in the laboratory furnaces, drying also eliminates capillarity-driven migration of water-soluble salts through the wet feed to the top surface of the sample, which would lead to undesirable non-uniformity in composition.

As demonstrated in this study, the discontinuity in the temperature history caused by drying the slurry and storing the feed at room temperature before further heat treatment can lead to an exchange of H₂O and CO₂ between the atmosphere and the dry samples, thus affecting the conversion process during the initial stages of melting. Using freshly prepared feeds and drying samples before heat treatment would eliminate this problem.

6. Conclusions

An understanding of the cold-cap reactions, although still incomplete, has been enhanced by the quantitative EGA via the TGA-GC-MS combination. The peaks identified by thermal analysis and represented by the kinetic model can thus be assigned to the evolving gases. Three different methods, based on stoichiometry, least squares, and calibration, gave rise to a linear relationship that correlates the overall mass loss rate from TGA with the sum of the production rates of individual gases from EGA. Future work could include identifying cold-cap reactions, including the reactants and the products.

Acknowledgements

This work was supported by the Department of Energy's Waste Treatment and Immobilization Plant Federal Project Office. Pavel Hrma was also partially supported by the World Class University program through the National Research Foundation of Korea funded by the Ministry of Education, Science and Technology (R31-30005). The authors are grateful to Drs. Dong-Sang Kim and Ekkehard Post for insightful discussions and instructions on the TGA-GC-MS setup and tests, respectively. Pacific Northwest National Laboratory is operated by Battelle Memorial Institute for the U.S. Department of Energy under contract DE-AC05-76RL01830.

References

- [1] R. Pokorný, P. Hrma, Mathematical modeling of cold cap, *J. Nucl. Mater.* 429 (2012) 245–256.
- [2] P. Hrma, A.A. Kruger, R. Pokorný, Nuclear waste vitrification efficiency: cold cap reactions, *J. Non-Cryst. Solids* 358 (2012) 3559–3562.
- [3] R. Pokorný, D.A. Pierce, P. Hrma, Melting of glass batch: model for multiple overlapping gas-evolving reactions, *Thermochim. Acta* 541 (2012) 8–14.
- [4] F.W. Wilburn, C.V. Thomasson, The application of differential thermal analysis and thermogravimetric analysis to the study of reactions between glass-making materials. Part 1. The sodium carbonate–silica system, *J. Soc. Glass Technol.* 42 (1958) 158T–175T.
- [5] C.V. Thomasson, F.W. Wilburn, The application of differential thermal analysis and thermogravimetric analysis to the study of reactions between glass-making materials. Part 2. The calcium carbonate–silica system with minor batch additions, *Phys. Chem. Glasses* 1 (1960) 52–69.

- [6] F.W. Wilburn, C.V. Thomason, The application of differential thermal analysis and thermogravimetric analysis to the study of reactions between glass-making materials. Part 3. The sodium carbonate–silica system, *Phys. Chem. Glasses* 2 (1961) 126–131.
- [7] F.W. Wilburn, C.V. Thomason, The application of differential thermal analysis and differential thermogravimetric analysis to the study of reactions between glass-making materials. Part 4. The sodium carbonate–silica–alumina system, *Phys. Chem. Glasses* 4 (1963) 91–98.
- [8] F.W. Wilburn, S.A. Metcalf, R.S. Warburton, Differential thermal analysis, differential thermogravimetric analysis, and high temperature microscopy of reactions between major components of sheet glass batch, *Glass Technol.* 6 (1965) 107–114.
- [9] E. Bader, Thermoanalytical investigation of melting and fining of Thüringen laboratory glassware, *Silikattechnik* 29 (1978) 84–87.
- [10] J. Mukerji, A.K. Nandi, K.D. Sharma, Reaction in container glass batch, *Ceram. Bull.* 22 (1979) 790–793.
- [11] O. Abe, T. Utsunomiya, Y. Hoshino, The reaction of sodium nitrate with silica, *Bull. Chem. Soc. Jpn.* 56 (1983) 428–433.
- [12] T.D. Taylor, K.C. Rowan, Melting reactions of soda-lime-silicate glasses containing sodium sulfate, *J. Am. Ceram. Soc.* 66 (1983) C227–C228.
- [13] M. Lindig, E. Gehrman, G.H. Frischat, Melting behavior in the system $\text{SiO}_2\text{--K}_2\text{CO}_3\text{--CaMg}(\text{CO}_3)_2$ and $\text{SiO}_2\text{--K}_2\text{CO}_3\text{--PbO}$, *Glastech. Ber.* 58 (1985) 27–32.
- [14] C.A. Sheckler, D.R. Dinger, Effect of particle size distribution on the melting of soda-lime-silica glass, *J. Am. Ceram. Soc.* 73 (1990) 24–30.
- [15] K.S. Hong, R.E. Speyer, Thermal analysis of reactions in soda-lime-silicate glass batches containing melting accelerants: I. One- and two-component systems, *J. Am. Ceram. Soc.* 76 (1993) 598–604.
- [16] K.S. Hong, S.W. Lee, R.E. Speyer, Thermal analysis of reactions in soda-lime-silicate glass batches containing melting accelerants: II. Multicomponent systems, *J. Am. Ceram. Soc.* 76 (1993) 605–608.
- [17] F. Krämer, Gasprofilmessungen zur bestimmung der gasabgabe beim glasschmelzprozeß, *Glastech. Ber.* 53 (1980) 177–188.
- [18] J. Chun, D.A. Pierce, R. Pokorný, P. Hrma, Cold-cap reactions in vitrification of nuclear waste glass: experiments and modeling, *Thermochim. Acta* 559 (2013) 32–39.
- [19] P.A. Smith, J.D. Vienna, P. Hrma, The effects of melting reactions on laboratory-scale waste vitrification, *J. Mater. Res.* 10 (1995) 2137–2149.
- [20] J. Matyáš, P. Hrma, D.-S. Kim, Melt Rate Improvement for High-Level Waste Glass, PNNL-14003, Pacific Northwest National Laboratory, Richland, Washington, 2002.
- [21] B. Roduit, J. Baldyga, M. Maciejewski, A. Baiker, Influence of mass transfer on interaction between thermoanalytical and mass spectrometric measured in combined thermoanalyzer-mass spectrometer systems, *Thermochim. Acta* 295 (1997) 59–71.
- [22] M. Maciejewski, A. Baiker, Quantitative calibration of mass spectrometric signals measured in coupled TA-MS system, *Thermochim. Acta* 295 (1997) 95–105.
- [23] C.-A. Craig, K.E. Jarvis, L.J. Clarke, An assessment of calibration strategies for the quantitative and semi-quantitative analysis of calcium carbonate matrices by laser ablation-inductively coupled plasma-mass spectroscopy (LA-ICP-MS), *J. Anal. At. Spectrom.* 15 (2000) 1001–1008.
- [24] M.J. Schweiger, P. Hrma, C.J. Humrickhouse, J. Marcial, B.J. Riley, N.E. TeGrotenhuis, Cluster formation of silica particles in glass batches during melting, *J. Non-Cryst. Solids* 356 (2010) 1359–1367.
- [25] P.R. Hrma, M.J. Schweiger, B.M. Arrigoni, C.J. Humrickhouse, J. Marcial, A. Moody, C. Rodriguez, R.M. Tate, B. Tincher, Effect of Melter-Feed-Makeup on Vitrification Process, PNNL-18374, Pacific Northwest National Laboratory, Richland Washington, 2009.
- [26] NIST 12 MS/MS Data base and Search Program. (see <http://chemdata.nist.gov/mass-spc/msms-search/>).
- [27] M.D. Dolan, S.T. Mixture, Analysis of glass batch reactions using *in situ* X-ray diffraction. Part III. Borosilicate glass batches, *Glass Technol.* 45 (2004) 212–219.
- [28] A. Monteiro, S. Schuller, M.J. Toplis, R. Podor, J. Ravaux, N. Clavier, H.P. Brau, T. Charpentier, F. Angeli, N. Leterrier, Chemical and mineralogical modifications of simplified radioactive waste calcine during heat treatment, *J. Nucl. Mater.* 448 (2014) 8–19.